



# Monitoring seagrass meadows in Maputo Bay using integrated remote sensing techniques and machine learning

M. Amone-Mabuto<sup>a,b</sup>, S. Bandeira<sup>a</sup>, J. Hollander<sup>c</sup>, D. Hume<sup>d</sup>, J. Campira<sup>a</sup>, JB Adams<sup>b,\*</sup>

<sup>a</sup> Department of Biological Sciences, Eduardo Mondlane University, Maputo, Mozambique

<sup>b</sup> Department of Botany, Institute for Coastal and Marine Research, Nelson Mandela University, PO Box 77000, Gqeberha, South Africa

<sup>c</sup> World Maritime University, Ocean Sustainability, Governance & Management Unit, Malmö, Sweden

<sup>d</sup> Department of Aquatic Resources, Swedish University of Agricultural Sciences, Sweden

## ARTICLE INFO

### Keywords:

Seagrass cover  
Extent change  
Aboveground biomass  
UAV systems  
Southern Mozambique

## ABSTRACT

Seagrass meadows are one of the most productive and valuable ecosystems on the planet. Monitoring seagrass meadows is essential to understand how these habitats change, and to develop better management and conservation practices. This study integrated satellite imagery from Sentinel-2 and Unmanned Aerial Vehicles (UAV) using machine learning to provide a consistent classification approach for monitoring seagrass in Maputo Bay, southern Mozambique. Sentinel-2 imagery was used to map seagrass extent and changes in Maputo Bay. The UAV systems were used to map seagrass at species level and biomass. All three algorithms tested in the ArcGIS environment could detect seagrass with high producer accuracy and Kappa coefficient. The area of seagrass in Maputo Bay decreased by 33.4 % between 1991 and 2023, with a decreasing trend of 0.48 km<sup>2</sup>/yr. A zonation pattern was observed for *Oceana serrulata* and *Zostera capensis* from the UAV imagery. The small and narrow leaved species (*Z. capensis*) occurred in the intertidal zone replaced by the broadleaved species (*O. serrulata*) in the subtidal. The total average aboveground biomass was 33.2 kg dry weight for the mapped area. The results of this study will guide implementation of combined satellite and UAV imagery with machine learning techniques for seagrass monitoring and restoration in Mozambique.

## 1. Introduction

Seagrass ecosystems provide a range of provisioning, regulating and cultural ecosystem services (Nordlund and Gullström, 2013, Amone-Mabuto et al., 2023) that contribute to human welfare and other goods and services (Findlay et al., 2011). The Mozambique coastline stretching over 2700 km, hosts one of the highest diversities of seagrass of the Western Indian Ocean region (Green and Short, 2003; Gullström et al., 2021). They are economically critical for coastal communities where fish, clams and crustaceans are collected, with 90 % of the national Gross Domestic Product (GDP) coming from artisanal fisheries (Poursanidis et al., 2021). However, they undergo changes in biomass and productivity continuously. The impact of natural disasters such as cyclones, floods (Amone-Mabuto et al., 2017; Bandeira et al., 2021), and the effects of higher sea-surface temperatures as well as sea level fluctuations (Solana et al., 2020; Asante et al., 2023) on seagrass ecosystems have been documented in the Maputo and Inhambane bays. Furthermore, destructive fishing practices including both semi-industrial

shrimp trawlers and artisanal beach seine netting are damaging seagrass habitats (Gullström et al., 2021). For example, in the Bazaruto Archipelago, despite being incorporated in an established Marine Protected Area (with both permanent and seasonal closures), seagrass meadows are heavily fished using beach-seine netting (D'Agata, 2016; Gullström et al., 2021). In the northwest region of Maputo Bay, large areas of *Zostera capensis* have disappeared where a previous seagrass cover of 60 % in 1991 decreased to just 10 % within a ten-year period (Bandeira et al., 2014). The main factors leading to this reduction included sedimentation from flooding around the 2000's and anthropogenic impacts due to digging for clam collection.

Seagrasses have varied morphologies (Duarte, 1991) and can respond differently to changes in the environment (Roca et al., 2016), therefore mapping their extent, composition and aboveground biomass (AGB) at species level is necessary to obtain accurate information to inform monitoring and restoration programmes. AGB is one of the key indicators of seagrass health (Vieira et al., 2018). It determines diversity and abundance of macroinvertebrates as well as the contribution of

\* Corresponding author.

E-mail address: [Janine.Adams@mandela.ac.za](mailto:Janine.Adams@mandela.ac.za) (J. Adams).

<https://doi.org/10.1016/j.rsma.2024.103816>

Received 27 May 2024; Received in revised form 10 September 2024; Accepted 14 September 2024

Available online 19 September 2024

2352-4855/© 2024 The Author(s). Published by Elsevier B.V. This is an open access article under the CC BY-NC license (<http://creativecommons.org/licenses/by-nc/4.0/>).

seagrass to carbon cycling which helps in the mitigation of climate change. For these reasons cover and AGB were investigated in this study.

Seagrass habitats can be mapped using different approaches, from *in situ* observations to remote sensing. Traditionally, *in situ* measurements such as boundary-tracking, transect or random-quadrat surveys have been used for direct seagrass mapping. These methods can provide accurate and precise results on seagrass species and percentage cover at a series of points. However, interpolation to calculate total area coverage can result in an overestimate for irregular meadows. In addition, these methods are time-consuming, and sometimes cannot be applied in remote areas. Remote sensing techniques have since been established as a facilitating and supporting method to gather information about ecosystems (Rommel et al., 2022). Several authors have effectively mapped seagrass meadow dynamics in shallow waters using remote sensing data such as Quickbird-2 (2.4×2.4 m), together with advanced image processing techniques, driven by machine learning algorithms (Pu et al., 2012; Calleja et al., 2017; Duffy et al., 2018; Astuty and Wicakson, 2019, Ivajnsiĉ et al., 2022, Lugendo et al., 2024). In Mozambique, only a few seagrass mapping efforts has been conducted, using mid-resolution satellite imagery such as Landsat 8, Sentinel-2 and Spot 5 (Ferreira et al., 2009; Ferreira et al., 2012; Ferreira and Bandeira, 2014; Bandeira et al., 2014; Amone-Mabuto et al., 2017; Poursanidis et al., 2021; Traganos et al., 2022). Such application is useful in large-scale mapping, but it is limited in terms of accuracy in capturing the very dynamic habitat features of seagrass meadows (Kutser et al., 2020; Lønborg et al., 2021; Hamad et al., 2022).

Unmanned aerial vehicle (UAV) techniques, are becoming popular platforms for spatial assessment of ecological phenomena (Anderson and Gaston, 2013; Klemas, 2015; Manfreda et al., 2018; Nahirnick et al., 2019; Singh and Frazier, 2018; Malerba et al., 2023). They are suitable to obtain images of very fine spatial resolution (0.01–5 cm) to detect changes in small patch and landscape features that would not be possible with satellite or aerial photography (Duffy et al., 2018; Yang et al., 2023) and generally have lower operational costs when mapping at such high spatial resolutions. UAVs have proven to be a suitable tool to map seagrass species based on machine learning algorithms (Román et al., 2021), to characterize the habitat conditions of shallow-water seagrass-dominated areas (Hamad et al., 2022), to estimate seagrass wrack carbon (Chen et al., 2023), or to quantify seagrass responses to disease and thermal stress (Aoki et al., 2023). Studies on applications of the UAV imagery to map seagrass to species biomass level are still scarce and have not yet been documented in Mozambique. Given the high ecosystem value of seagrass meadows and the usefulness of these habitats for marine ecosystem health (Roca et al., 2016; Purvaja et al., 2018) establishing a reliable, rapid, and cost-effective mapping approach to aid seagrass monitoring programs is indispensable (Duffy et al., 2018; Hamad et al., 2022).

Some studies have shown that object-based image analysis (OBIA) approaches outperform pixel-based approaches when classifications are based on very high-resolution data (Dronova, 2015; Mahdavi et al., 2017), and machine learning algorithms provide different ways of classifying these objects (Rommel et al., 2022). Random Trees (RT), Support Vector Machine (SVM) and Maximum Likelihood (ML) are some algorithms that have been used to map seagrass habitats with good results (Villoslada et al., 2020; Ivajnsiĉ et al., 2022; Hamad et al., 2022; Benmokhtar et al., 2023). The performance of the algorithms depends on the classes being mapped, the training data and the predictor variables provided, thereafter, multiple classifiers should be tested to identify the best option (Maxwell et al., 2018). The aim of this study was to compare the classification results of Random Tree (RT), Support Vector Machine (SVM), and Maximum Likelihood methods using Sentinel-2 and UAV images to map seagrass extent and species biomass, and evaluate changes in seagrass extent in Maputo Bay, southern Mozambique. These data will inform seagrass monitoring and restoration in Mozambique. As seagrasses are increasingly recognised for their potential carbon stocks and sequestration (Poursanidis et al., 2021),

they have been included in the Nationally Determined Contributions to strengthen the country's action plans to mitigate climate change. Therefore, measuring the health and distribution of seagrasses is critical to understanding their role in carbon sequestration and monitoring climate change targets.

## 2. Materials and Methods

### 2.1. Study site

Maputo Bay (Fig. 1A) is in southern Mozambique between 25°72'–26°28'S, 32°40'–32°85'E and has a water surface area of approximately 1100 km<sup>2</sup> (Guissamulo and Cockcroft, 2004). The Bay has an average depth of 10 m, except for the northern part near the entrance to the Indian Ocean, where depths can reach up to 18–23 m (Amone-Mabuto et al., 2023). The tide is semi-diurnal, with an average spring and neap tidal range between 3.0 and 1.0 m respectively. Nine seagrass species have been identified in Maputo Bay including *Thalassia hemprichii* (Ehrenberg) Ascherson, *Halodule uninervis* (Forskål) Ascherson, *Thalassodendron ciliatum* (Forskål) den Hart, *Oceana serrulata* (R. Brown) Byng & Christenhusz, *Cymodocea rotundata* Ehrenberg & Hempr. Ex Ascherson, *Halophila ovalis* (R.Br.) Hooker f., *Syringodium isoetifolium* (Ascherson) Dandy, *Zostera capensis* Setchell and *Thalassodendron leptocaula* Maria C. Duarte, Bandeira & Romeiras (Bandeira et al., 2014). These species occur in a range of community types, from monospecific stands to mixed communities with one or two dominant seagrass species (Bandeira et al., 2014; Gullström et al., 2021; Amone-Mabuto et al., 2022) occurring mainly in shallow inlets bordering Inhaca Island (Ferreira and Bandeira, 2014). In Bairro dos Pescadores, north of Maputo City, only four species occur and *Z. capensis* is dominant. Frequent disturbance from clam collection has reduced the seagrass extent. A large bay is situated in the southern part of Inhaca Island (Fig. 1B), that has a range of habitats including mangrove forest in Saco, coral reef in Ponta Torres and mudflats and seagrass beds in the Banco area, in the middle of the bay. The Banco area (Fig. 1C) is an important fishing ground for the local community, where fish, shellfish and crabs are caught in considerable quantities (de Boer, 2000).

### 2.2. Seagrass mapping and change detection

#### 2.2.1. Maps of seagrass cover - 2023

To create the seagrass cover maps for 2023 a Sentinel-2 (Level 1 C) image of Maputo Bay captured on July 4, 2023, was selected for its minimal cloud cover (Cloud cover percentage: 1.2 % and Cloud shadow percentage: 0.03 %) and downloaded from the Copernicus Open Access H (<https://scihub.copernicus.eu/dhus/#/home>) (Table 1). Only the visible range Bands 2 (blue), 3 (green) and 4 (red), were used to build the RGB composite image, since they penetrate the water column more deeply and thus provide sensitive quantitative data on bottom reflectance (Ivajnsiĉ et al., 2022). The image was clipped of the areas of interest separately (Inhaca Island and Bairro dos Pescadores) to focus only on the shallow coastal part of the bay, where seagrass meadows are commonly present. A satellite image mask was used to remove any cloud shadow thus enhancing the coastal water features. Water column correction was not applied on the single image, since it is known to have limited effectiveness in shallow waters (up to depth of 3 m) (Uhrin and Townsend, 2016) and it has been demonstrated that Sentinel-2 data can achieve benthic substrate differentiation through atmospheric correction only (Kuhwald et al., 2021; Li et al., 2023). Several points were drawn to represent sand and shallows water (classified as others) using the Sentinel image and ArcGIS Pro (version 2.8) world imagery layer sourced from Maxar data at 1.0 m resolution (from 3 May 2023).

#### 2.2.2. Image classification

The RGB composite image was the source for supervised image classification techniques in ArcGIS 10.50. The classification was

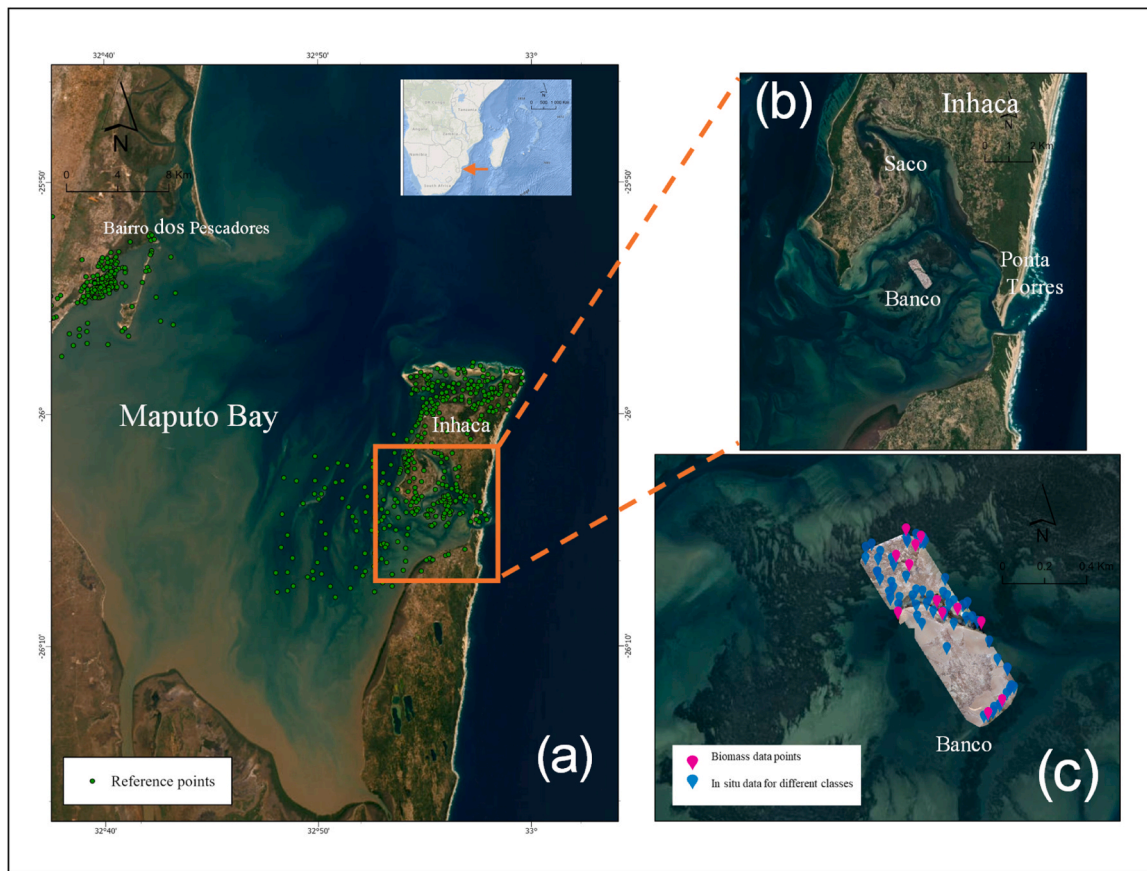


Fig. 1. The study area of Maputo Bay, with a) the spatial distribution of reference data points across Inhaca Island and Bairro dos Pescadores b) RGB UAV image from the Banco area of the southern bay of Inhaca Island and c) pink and blue pins depict location of field data points.

Table 1  
Spectral characteristics of the Sentinel-2 satellite image used in the study.

Band No.	Spectral Band	Central Wavelength ( nm )	Spatial Resolution ( m )
1	Coastal aerosol	442	60
2	Blue	495	10
3	Green	582	10
4	Red	664	10
5	Vegetation red edge	703	20
6	Vegetation red edge	739	20
7	Vegetation red edge	779	20
8	Near Infra-Red (NIR)	883	10
8 A	Narrow NIR	864	20
9	Water vapor	943	60
10	Cloud cirrus	1377	60
11	Short Wave Infra-Red (SWIR)	1610	20
12	Short Wave Infra-Red (SWIR)	2186	20

Table 2  
Dataset used in the machine learning for object-based image analysis.

	Inhaca Island	Bairro dos Pescadores
<b>Training data</b>		
Seagrass	386	243
Others	521	306
<b>Validation data</b>		
Seagrass	156	100
Others	239	156

supported by several training polygons (representing 69.1 % of the data set) determined on object-based image analysis (OBIA) (Table 2). Two different categories were distinguished including *seagrasses*, with sand banks, rocks, coral, shallow waters, mangrove, considered as *others*. To assure the best possible estimate of seagrass cover in 2023, three algorithms in the ArcGIS environment (ESRI, 2020) were applied: (1) the Random Trees (RT), (2) the Support Vector Machine (SVM) and (3) the Maximum Likelihood (ML) (Fig. 2). A detailed explanation of these classification algorithm is given in Otukei and Blaschke (2010). The classification algorithms were trained using a subset of those training data to obtain a model to be applied. Afterwards, the recognition of different categories was carried out by applying each model to the whole image window (Medina and Atehortúa, 2019). Finally, the validation phase of the obtained results was performed.

### 2.2.3. Accuracy assessment

Quantifying the amount of error in a classified image is crucial to reach the best link between image and reality (Ivajnsić et al., 2022). Thus, the results were used for accuracy assessment based on the confusion matrix for each image classification algorithm. A separate data set not used for training was used for accuracy assessment (30.9 %) with a total of 651 validation points for both classes (*seagrass* and *others*) at Inhaca and Bairro dos Pescadores. The data set was produced based on the knowledge and experience from manual image interpretation and several seagrass image pixels (Li et al., 2023). We validated the accuracy of the seagrass ecosystem cover using the following statistical metrics: producer accuracy (PA), overall accuracy (OA), user accuracy (UA) and Kappa coefficient (Kc). OA shows the proportion of validation data that were classified correctly. PA indicates how often real objects of a class on the ground are correctly shown on the resulting classification map,

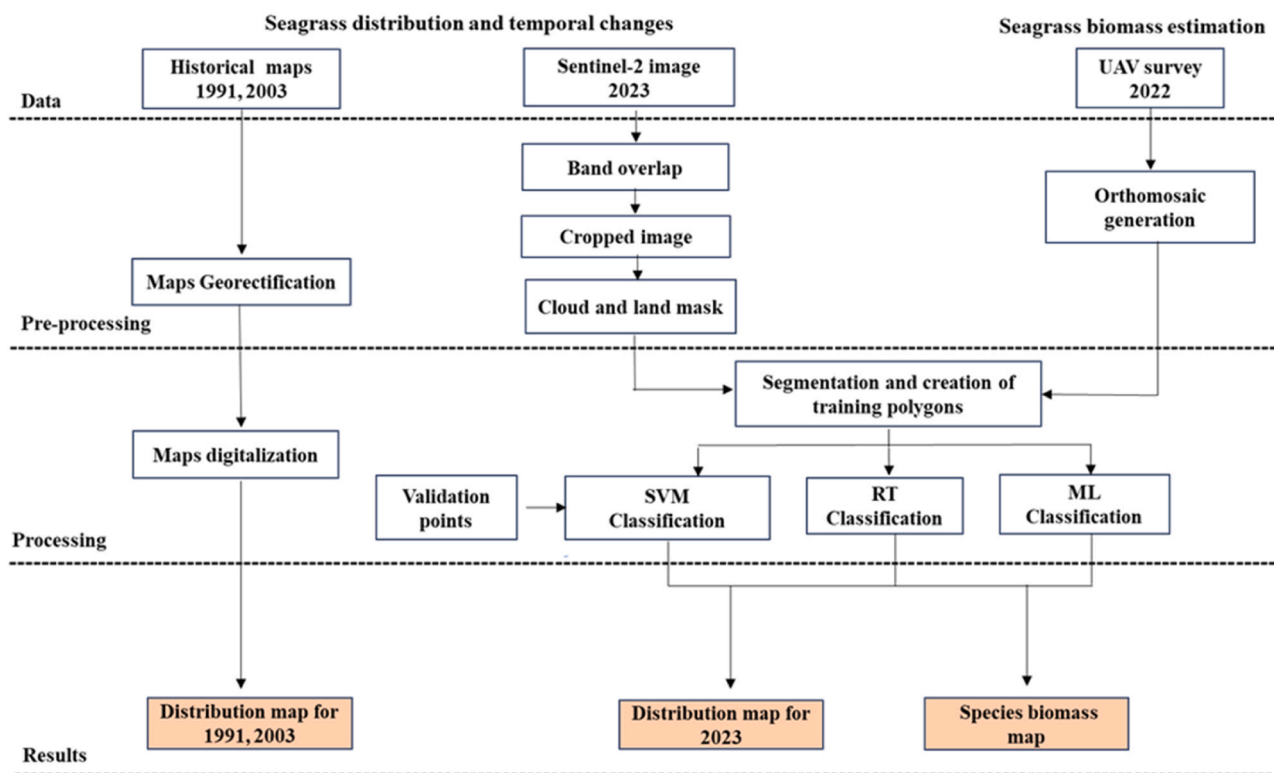


Fig. 2. Schematic overview of the methodological framework applied to map seagrass distribution and biomass.

while UA indicates how often a class on the resulting classification map will be present on the ground. Kc compares classification results to values assigned by chance (Congalton and Green, 2019).

#### 2.2.4. Change analysis

The remote sensing part of this study was performed with the purpose of updating the seagrass distribution map of Maputo Bay. This update aimed to evaluate the temporal dynamics of seagrass meadows along the bay compared to the historical seagrass distribution maps from 1991 and 2003 (Bandeira et al., 2014). To achieve this, the historical maps were scanned and georectified as a prerequisite to digitizing polygons (Knowles and Hillier, 2008; Novak and Ostash, 2022) in ArcGIS software. The seagrass cover status in 1991 and 2003 were based on satellite images and extensive ground truthing. We test the assumption that seagrass habitats have been losing extent in recent years mainly in Bairro dos Pescadores, northwest Maputo Bay. The historical maps were compared against the remote sensing product from 2023. The change analysis should be considered as an estimation with a certain level of certainty; 93 % and 85 % for Inhaca Island and Bairro dos Pescadores respectively for the SVM algorithm.

### 2.3. Aboveground biomass estimation

#### 2.3.1. UAV data collection

We deployed two Phantom 4 Pro multirotor drones with onboard GPS for georeferencing in the Banco area of the southern bay of Inhaca Island (an area dominated by *Z. capensis*) with the prior flight missions planned on Pix4Dcapture app. The front- and side-image overlaps were set to 80 % in all the flights to increase the alignment accuracy. The drones were flown at a 65-m altitude in 15 flights (Table 3), which resulted in the ground image spatial resolution of 1.64 cm and with flight speed not exceeding  $15 \text{ m}\cdot\text{s}^{-1}$ . The mapping was performed during low tide, where both parallel and perpendicular orientations to the coastline were applied, primarily based on the orientation of the distribution of the seagrasses. All images were taken with the camera facing

Table 3

Details of UAV flights for the study area.

Location	Date	Number of flights	Number of images	Flight altitude (m)
Southern Inhaca	17/02/2022–28/02/2022	15	7928	65

down, to ensure camera position was associated with the centre of the image (Price et al., 2022).

#### 2.3.2. UAV image processing and classification

Pix4DMapper (Version 1.6.6) was used to create mosaics of the drone imagery, using a scale-invariant feature transformation algorithm to detect features for matching images. High quality alignment was chosen to utilise the full image resolution. We chose one orthomosaic derived from 334 images to process the classification. The remaining data were stored for further analysis. The orthomosaic was exported in GeoTIFF format into ArcGIS for subsequent OBIA processing. A supervised classification scheme was employed to categorize image pixels into different classes. We manually selected a set of image objects as training samples to train the three algorithms (SVM, RT and ML). The confusion matrix for each image classification algorithm were also computed in the ArcGIS environment (ESRI, 2020). The matrices were built using *in situ* data points collected and visually inspected on the original true colour orthomosaic (Fig. 3). Due to the ultra-high spatial resolution, visual photo interpretation could be considered very reliable for assessing the accuracy of thematic maps (Lechner et al., 2012; Ventura et al., 2023). The accuracy assessment was measured using four indicators: producer accuracy, overall accuracy, Kappa coefficient and user accuracy. The best performing seagrass species classification algorithm was selected for total AGB estimation.

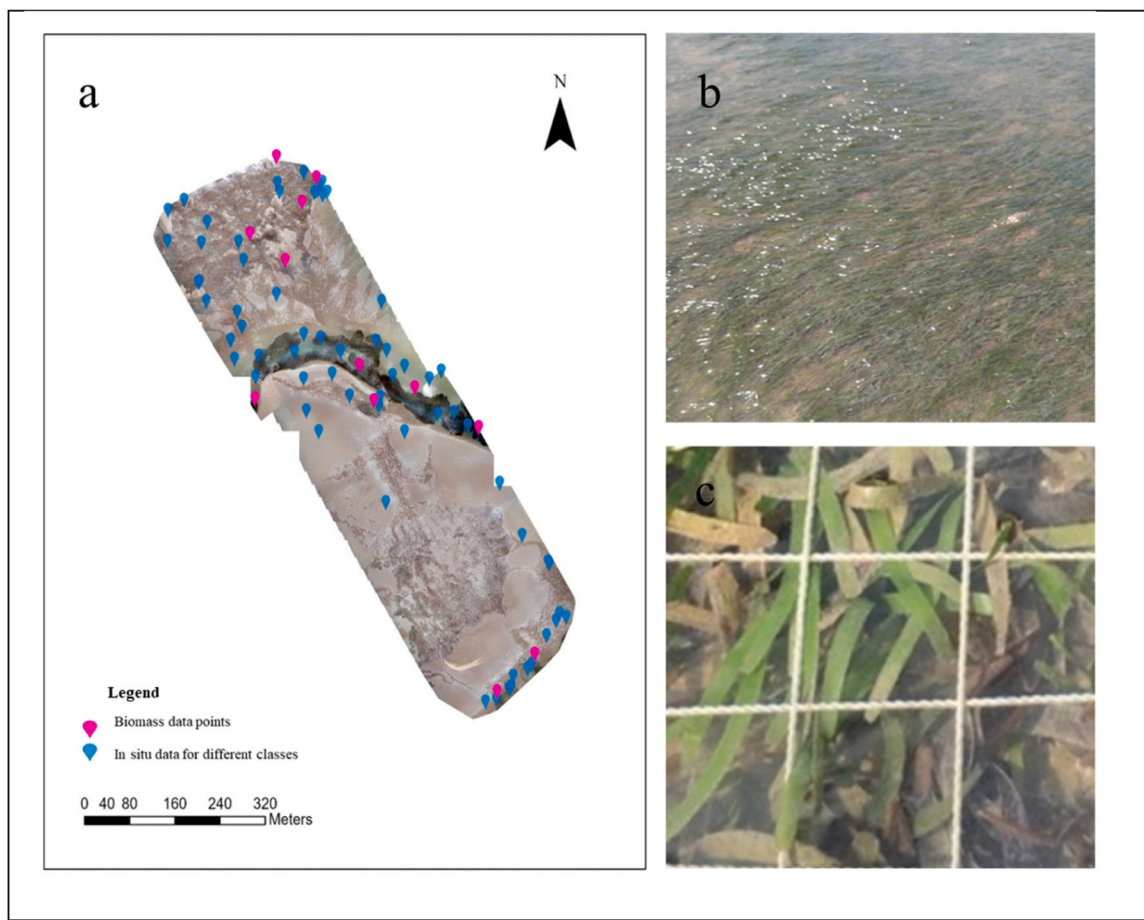


Fig. 3. UAV orthomosaic used for seagrass species map and aboveground biomass estimation (a) Seagrass *Z. capensis* (b) and *O. serrulata* (c) sampled in the study area.

Table 4  
In situ benthic classes sampling points.

Class	Points	%
<i>Oceana serrulata</i>	18	23.4
<i>Zostera capensis</i>	16	20.8
Bare sand	33	42.8
Water	10	13.0
<b>Total</b>	<b>77</b>	<b>100</b>

2.3.3. In situ measurements

In situ measurements were randomly carried out at 77 points (Fig. 3, Table 4) to determine the different benthic classes and seagrass species. In the surveyed area we found four of the nine seagrass species reported for Inhaca Island, namely *Halodule uninervis*, *Thalassia hemprichii*, *Oceana serrulata* and *Zostera capensis*, the last two being the dominant species in terms of abundance. Percentage cover of the dominant species was assessed in 12 quadrats of 50 × 50 cm following McKenzie et al., (2001). In addition, 12 small quadrats (25 × 25 cm) were used for the measurement of AGB (Gokulakrishnan and Ravikumar, 2016). Seagrass biomass was collected with a spade to the depth of root penetration, cleaned from sediment with seawater, put in an ice box and taken to the laboratory. Subsequently, the samples were washed with fresh water and any epiphytes attached to the seagrass was removed. The samples were separated into aboveground (leaves) and belowground biomass (roots and rhizomes) and dried in an oven at a fixed temperature of 80 °C for 48 hours, then weighed to measure the dry weight (only AGB data were used in this study). The values of dry weight were converted to an area of a square meter (Table 5) by dividing the dry weight of each

Table 5  
Seagrass aboveground biomass in each quadrat and aboveground biomass converted to square meters (m<sup>2</sup>).

Quadrat	Species	Substrate type	Cover (%) 50 cm <sup>2</sup>	AGB (g. DW)	AGB (g.DW/m <sup>2</sup> )
1	<i>O. serrulata</i>	Sand	85	18.13	290.06
2	<i>O. serrulata</i>	Sand	95	19.98	319.70
3	<i>O. serrulata</i>	Sand	100	20.94	335.07
4	<i>O. serrulata</i>	Sand	95	20.77	332.38
5	<i>O. serrulata</i>	Sand	90	18.32	293.13
6	<i>O. serrulata</i>	Sand	95	20.11	321.81
7	<i>Z. capensis</i>	Sand and Mud	70	12.41	198.61
8	<i>Z. capensis</i>	Sand and Mud	60	11.82	189.19
9	<i>Z. capensis</i>	Mud	85	13.37	213.86
10	<i>Z. capensis</i>	Mud	95	13.87	221.88
11	<i>Z. capensis</i>	Mud	95	13.77	220.32
12	<i>Z. capensis</i>	Sand and Mud	45	11.78	188.48

sample by the quadrat size. The total AGB (measured in dry weight (DW)) for each species was obtained following Chayhard and Buranapratheprat (2018), by multiplying the average AGB of the species by the area covered by the species. Regression linear analysis between AGB and UAV RGB bands and between percentage cover and UAV RGB bands were performed to understand how the bands are correlated to the in situ measurements. Regression analysis was also determined between AGB and percentage cover.

### 3. Results

#### 3.1. Seagrass mapping and change detection

The 2023 mapping produced from the RGB composite classification revealed that seagrasses cover 30.63 km<sup>2</sup> along the Maputo Bay with 30.07 km<sup>2</sup> at Inhaca Island (Fig. 4C) and 0.56 km<sup>2</sup> at Bairro dos Pescadores (Fig. 4F). The seagrass distribution maps obtained by classification using the OBIA method were effective in providing an overview of the main extent. Accuracy measures using different algorithms are presented in Table 6. The results showed that the assessment values were different for each image, but all presented a good OA and Kc value. The SVM algorithm presented the highest classification performance for Inhaca Island (the OA = 97 % and Kc = 0.93), compared with an OA = 93 % and Kc = 0.85 for Bairro dos Pescadores (OA = user accuracy and Kc = Kappa coefficient).

The seagrass meadow area decreased by 12.8 % (from 46.06 km<sup>2</sup> to 40.16 km<sup>2</sup>) between 1991 and 2003, followed by another decline of

23.7 % (from 40.16 km<sup>2</sup> to 30.63 km<sup>2</sup>) between 2003 and 2023 (Fig. 4 and Table 7). Overall, the area of seagrasses in the Maputo Bay decreased by 33.4 % between 1991 and 2023, with a decreasing trend of 0.48 km<sup>2</sup>/yr. Bairro dos Pescadores had the greatest decrease (86.3 %) in extent between 1991 and 2003 (Table 7). The distribution pattern of seagrass also appears to have changed over time at Inhaca Island. In 1991, the meadows were similarly abundant in the northern and southern bays. Declines up until 2023 mostly reflected losses from the southern meadows in the *Zostera capensis* dominated meadows (Fig. 4C).

#### 3.2. Aboveground biomass mapping

Two classes of dominant species (*Oceana serrulata* and *Zostera capensis*) were classified using SVM, RT and ML algorithms. The total seagrass area mapped was 0.000126 km<sup>2</sup> and the percentage of seagrass cover ranged from 0 % to 100 %. *Oceana serrulata* commonly grew in subtidal areas where it is constantly submerged at low tide. Its wide leaves created different reflectance compared with the thin *Z. capensis*



Fig. 4. Change detection in seagrass cover along Inhaca Island (a) in 1991, (b) 2003 and (c) 2023 and Bairro dos Pescadores with a focus on the *Zostera capensis* community (d) in 1991, (e) 2003, and (f) 2023.

**Table 6**  
Confusion matrices for seagrass mapping in Maputo Bay.

Inhaca Island					Bairro dos Pescadores			
SVM	Seagrass	Other	Total	UA	Seagrass	Other	Total	UA
Seagrass	147	9	156	0.94	96	4	100	0.96
Other	4	235	239	0.98	14	142	156	0.91
Total	151	244	395		110	146	256	
PA	0.97	0.96			0.87	0.97		
OA	0.97				0.93			
Kc	0.93				0.85			
RT	Seagrass	Other	Total	UA	Seagrass	Other	Total	UA
Seagrass	122	34	156	0.78	97	3	100	0.97
Other	4	235	239	0.98	25	131	156	0.84
Total	126	269	395		122	134	256	
PA	0.97	0.87			0.80	0.98		
OA	0.90				0.89			
Kc	0.79				0.78			
ML	Seagrass	Other	Total	UA	Seagrass	Other	Total	UA
Seagrass	140	16	156	0.90	88	11	99	0.89
Other	6	233	239	0.98	11	145	156	0.93
Total	146	249	395		99	156	255	
PA	0.96	0.94			0.89	0.93		
OA	0.94				0.91			
Kc	0.88				0.82			

**Table 7**  
Seagrass cover and percentage loss at Inhaca Island and Bairro dos Pescadores between 1991 – 2023.

Site	Inhaca Island			Bairro dos Pescadores		
	1991	2003	2023	1991	2003	2023
Seagrass area (km <sup>2</sup> )	40.74	39.43	30.07	5.32	0.73	0.56
Seagrass cover lost (%)	<u>1991–2003</u>		<u>2003–2023</u>	<u>1991–2003</u>		<u>2003–2023</u>
	3.2 %		23 %	86.3 %		23.3 %

leaves occurring in intertidal areas which are exposed at low tides. The accuracy assessment showed that all algorithms were capable of distinguishing seagrass species (Fig. 5). SVM yielded a slightly higher mean overall accuracy of 89 % (Table 8).

The mean AGB of *O. serrulata* and *Z. capensis* were 315 g DW.m<sup>-2</sup> and 213 g DW.m<sup>-2</sup> respectively (Fig. 6) and the average AGB of the seagrass zone was 9.1 kg DW for *O. serrulata* and 20.7 kg DW for *Z. capensis*. The total average AGB for this area was 33.2 kg DW. The correlation

between total AGB, percentage cover and UAV RGB bands is shown in Fig. 7. The correlation between AGB and percentage cover of all species and of the two dominant species, *O. serrulata* and *Z. capensis* is shown in Fig. 8. The results indicated a low correlation between the AGB and the RGB band (R<sup>2</sup> = 0.35–0.49) and between the percentage cover and the RGB bands (R<sup>2</sup> = 0.13–0.21). Overall, RGB bands showed a linear relationship with AGB and percentage cover. The higher the RGB value, the closer the AGB or percent cover is to zero (absence of seagrass). In contrast, the results showed a moderate relationship (R<sup>2</sup> = 0.51) between AGB and percentage cover and a good relationship (R<sup>2</sup> = 0.85–0.94) when species were analysed separately.

#### 4. Discussion

##### 4.1. Advantages and disadvantages of classification algorithms

In this study, we have demonstrated the use of machine-learning approaches to successfully classify seagrass from Sentinel-2 images of Maputo Bay with the results then used to detect change in seagrass cover over a period of 32 years. The SVM, RT and ML algorithms were all

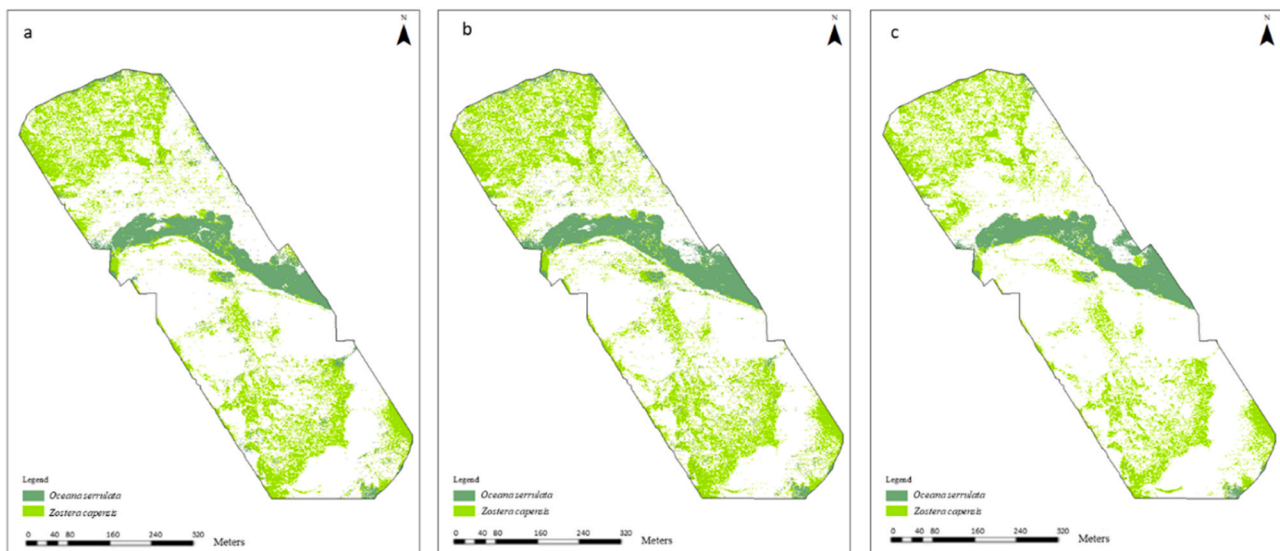


**Fig. 5.** UAV classification maps from SVM (a), RT (b) and ML (c).

**Table 8**  
Error matrices summary for the UAV image classification.

SVM	<i>O. serrulata</i>	<i>Z. capensis</i>	Other	Total	UA
<i>O. serrulata</i>	18	1	2	21	0.86
<i>Z. capensis</i>	0	16	6	22	0.73
Other	0	1	44	45	0.97
Total	18	18	52	88	
PA	1.00	0.89	0.85		
OA	0.89				
Kc	0.81				
RT	<i>O. serrulata</i>	<i>Z. capensis</i>	Other	Total	UA
<i>O. serrulata</i>	18	3	6	27	0.67
<i>Z. capensis</i>	0	14	2	16	0.88
Other	0	1	44	45	0.98
Total	18	18	52	88	
PA	1.00	0.78	0.86		
OA	0.86				
Kc	0.77				
ML	<i>O. serrulata</i>	<i>Z. capensis</i>	Other	Total	UA
<i>O. serrulata</i>	17	1	6	24	0.71
<i>Z. capensis</i>	1	16	4	21	0.76
Other	0	1	42	43	0.98
Total	18	18	52	88	
P	0.94	0.89	0.81		
A					
OA	0.85				
Kc	0.76				

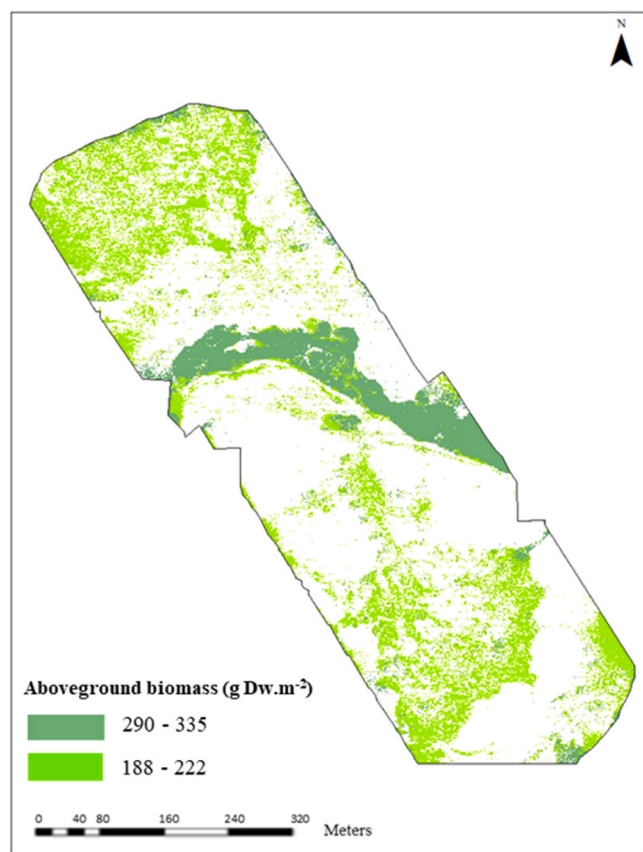


**Fig. 6.** Aboveground seagrass biomass estimated from the UAV image.

capable of detecting seagrass with high producer accuracy and Kappa coefficient. A previous study (Ivajnsić et al., 2022), tested these three algorithms for seagrass classification using Sentinel-2 imagery in the Adriatic Sea, with overall accuracies of 56–60 %. Koedsin et al., (2016), also tested the ML using higher resolution Worldview-2 (WV-2) imagery to map seagrass species cover and biomass in Southern Thailand with an overall accuracy of 90.7 %. However, both studies showed lower

accuracies than presented in this study. Although our study presented higher accuracy than previous studies of seagrass beds, it is difficult to compare the accuracy with other studies due to the environmental differences, variation in seagrass depth occurrence as well as the sensors used. Among the machine learning ensemble approaches used, RT and ML algorithms performed less well than SVM in both satellite and UAV imagery. These results are in line with that of Traganos and Reinartz (2018), who also compared the performance of SVM and RT in satellite imagery for *Posidonia oceanica* mapping and contradicts the superior performance of RT in other studies (Bakirman and Gumusay, 2020). In fact, SVM has high accuracy in handling complex and high-dimensional data, which makes it well suited for distinguishing seagrass from other types of classes, however this may not be suitable for large datasets with many features. Overall, the advantage of using machine learning algorithms is that they can process geospatial data more accurately than traditional methods. Machine learning algorithms can identify patterns and trends in data that may be difficult for humans to detect, resulting in more accurate analysis and predictions.

#### 4.2. Current status and changes in seagrass area

In 1991, there were extensive seagrass meadows in Maputo Bay (Bandeira, 2002; Bandeira et al., 2014). However, between 1991 and 2003, the meadows suffered a severe decrease in size mainly at Bairro dos Pescadores (northwest of the Maputo Bay). The main factors leading to this reduction included sedimentation from flooding around the 2000s and anthropogenic impacts due to digging for clam collection (Bandeira et al., 2014). From 2003–2023, the decline (about 23 %) was similar for Inhaca Island and Bairro dos Pescadores, with the meadows at Bairro dos Pescadores very sparse and patchy due to continuous digging for clam collection. Although Inhaca Island is located within the Maputo National Park, it is experiencing an increase in the number of tourists, especially during the peak season. The rapid urbanization for socio-economic development and the disturbance caused by boat traffic are leading to the destruction of seagrass ecosystems. This fact highlights that at the local scale, anthropogenic disturbance plays a major role in the survival of seagrass meadows.

#### 4.3. Seagrass biomass mapping

Monitoring seagrass AGB is crucial as it serves as a fundamental indicator of the productivity, biodiversity, and carbon storage of seagrass ecosystems. UAV imagery is suitable for detecting seagrass species in monospecific beds that occur in shallow waters. The images in this study were taken at an altitude of 65 m at low tide, providing a good spatial resolution of 1.64 cm/pixel and allowing different seagrass species to be clearly observed. From the UAV imagery we observed that different species grow in different locations. The zonation followed a pattern of small and narrow-leaved species in the intertidal zone (e.g. *Z. capensis*) being replaced by broad-leaved species in the subtidal zone (*O. serrulata*). In the intertidal flats this is an adaptation to tolerate prolonged exposure to high temperatures and desiccation. As a group, seagrasses span a wide range of morphological traits, growth patterns, physiology, and other life history traits (Short et al., 2007; Kilminster et al., 2015), making them differentially able to cope with environmental stress and competition (Rao et al., 2023).

The study showed that seagrass AGB was directly proportional to the seagrass percentage cover, which means the healthier the seagrass, the higher the AGB. Seagrass biomass also varied according to sediment type. Seagrass growing on muddy-sandy substrate had lower AGB, while seagrass growing on sandy substrate had higher AGB. Mallombasi et al., (2020) also found similar results investigating the relationship between seagrass *Thalassia hemprichii* percentage cover and their biomass.

The RGB bands from the UAVs showed high variability, despite the linear relationship with AGB and percent cover. This demonstrated the sensitivity to noise of environmental parameters such as reflectance. The

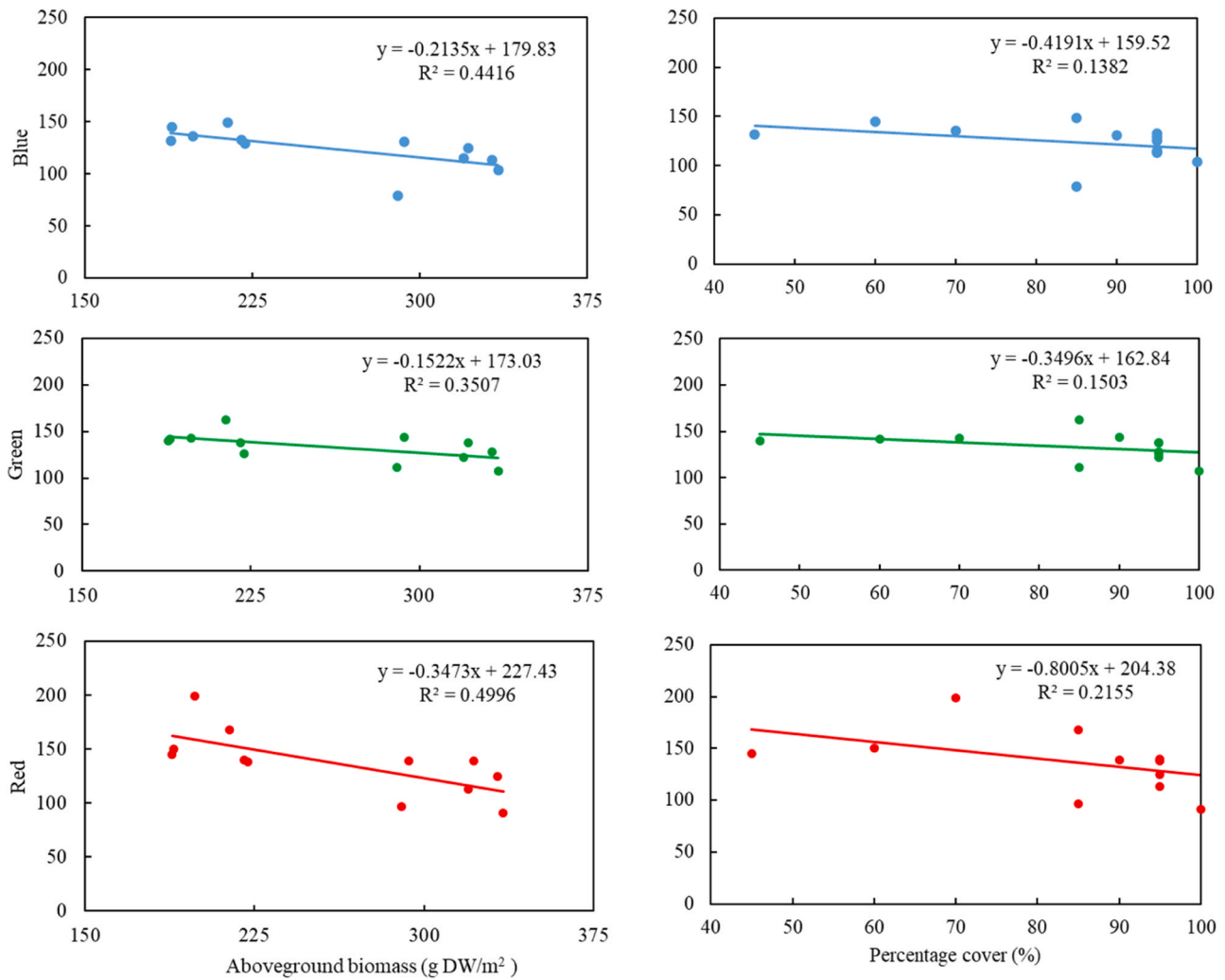


Fig. 7. RGB/in situ measurement plots showing the relationship between the value of the three UAV RGB bands and the seagrass aboveground biomass and percentage cover.

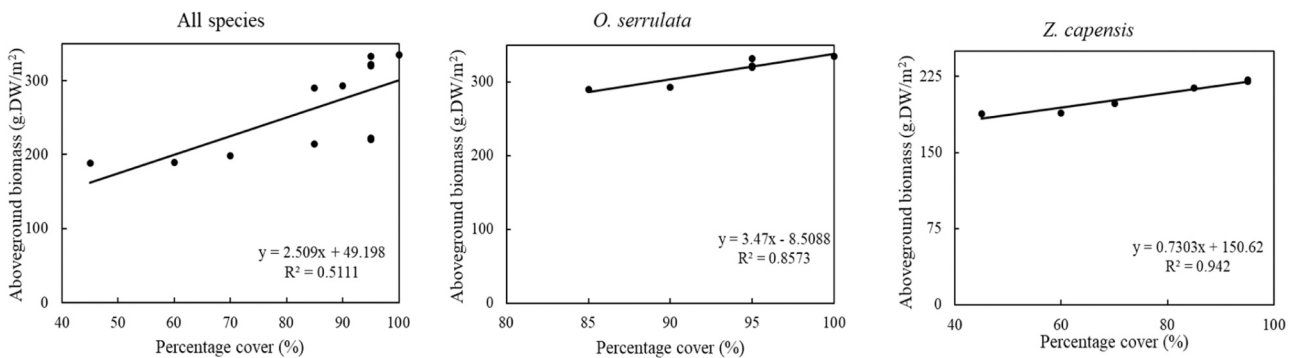


Fig. 8. Plots showing the relationship between seagrass aboveground biomass and percentage cover.

colour of the benthic classes can be disturbed by sea surface reflections and shadows, creating noise in the classification process. In fact, an automatic classifier requires an extensive *a posteriori* filtering process, which does not always define the class boundaries correctly (Apicella et al., 2023). We therefore propose the use of RGB imagery as validation data in satellite imagery for mapping seagrass AGB with manual digitization of the different classes using visual recognition of the benthic classes. Visual interpretation is more accurate as the human eye can detect a pattern and texture better than supervised classification. The

approach of our study can be used to retrieve information about the ecological status of seagrass to support management and restoration actions.

### 5. Conclusion

Seagrass meadows can be mapped successfully using Sentinel-2 and UAV imagery with high spatial resolution. In this study we proposed the combination of an object-based image analysis of UAV imagery with

satellite data and machine learning techniques for seagrass monitoring. The high spatial resolution and the flexible timing of image acquisition of UAVs can provide accurate training data, serving as a cost-effective supplement to ground truth data collected through field surveying. UAV surveys are constrained by flight duration and area coverage, limiting the areas to be monitored, thus, the combination of UAV and satellite data, set a promising path towards remote sensing-based monitoring. By combining the Sentinel-2 satellite images with UAV data, the extent and AGB of seagrass meadows can be monitored and accurately assessed balancing the different characteristics of the input images.

### Declaration of Competing Interest

The authors declare the following financial interests/personal relationships which may be considered as potential competing interests: Manuela Amone-Mabuto reports financial support was provided by MASMA. Manuela Amone-Mabuto reports financial support was provided by United Nations Environment Programme. If there are other authors, they declare that they have no known competing financial interests or personal relationships that could have appeared to influence the work reported in this paper.

### Data Availability

Data will be made available on request.

### Acknowledgments

This study was jointly funded by MASMA “Seagrass Protect”/WIOMSA (Grant Number: MASMA/OP/2018/02) and WIOSAP/UNEP (ID 4940. SSFA/2019/2480). DSI/NRF Research Chair in Shallow Water Ecosystems (UID 84375) supported JBA. Dr Rui Santos (University of Algarve) is acknowledged for his kind support in this study. JH would like to express his gratitude to the Nippon Foundation of Japan for their generous support.

### References

- Aoki, L.R., Yang, B., Graham, O.J., Gomes, C., Rappazzo, B., Hawthorne, T.L., Duffy, J.E., Harvell, D., 2023. UAV high-resolution imaging and disease surveys combine to quantify climate-related decline in seagrass meadows. *Oceanogr.* 36, 38–39. (<https://doi.org/10.5670/oceanogr.2023.s1.12>).
- Amone-Mabuto, M., Bandeira, S., Da Silva, A., 2017. Long-term changes in seagrass coverage and potential links to climate-related factors: the case of Inhambane Bay, southern Mozambique. *West. Indian Ocean J. Mar. Sci.* 16, 13–25.
- Amone-Mabuto, M., Hollander, J., Lugendo, B., Adams, J.B., Bandeira, S., 2022. A field experiment exploring disturbance-and-recovery, and restoration methodology of *Zostera capensis* to support its role as a coastal protector. *Nord. J. Bot.* 1, e03632. <https://doi.org/10.1111/njb.03632>.
- Amone-Mabuto, M., Mubai, M., Bandeira, S., Shalli, M., Adams, J.B., Lugendo, B., Hollander, J., 2023. Coastal communities' perception on the role of seagrass ecosystems for coastal protection and implications for management. *Ocean Coast. Manag.* 244, 106811. <https://doi.org/10.1016/j.ocecoaman.2023.106811>.
- Anderson, K., Gaston, K.J., 2013. Lightweight unmanned aerial vehicles will revolutionize spatial ecology. *Front. Ecol. Environ.* 11, 138–146. <https://doi.org/10.1890/120150>.
- Apicella, L., De Martino, M., Ferrando, I., Quarati, A., Federici, B., 2023. Deriving coastal shallow bathymetry from Sentinel 2-, Aircraft-and UAV-Derived orthophotos: a case study in Ligurian Marinas. *J. Mar. Sci. Eng.* 11, 671. <https://doi.org/10.3390/jmse11030671>.
- Asante, F., Bento, M., Broszeit, S., Bandeira, S., Chitara-Nhandimo, S., Amone-Mabuto, M., Correia, A.M., 2023. Marine macroinvertebrate ecosystem services under changing conditions of seagrasses and mangroves. *Mar. Environ. Res.* 189, 106026. <https://doi.org/10.1016/j.marenvres.2023.106026>.
- Astuty, L.S., Wicakson, P., 2019. Seagrass species composition and aboveground carbon stock mapping in Parang Island using Planetscope image. *Sixth Geoinf. Sci. Symp.* 11311, 1131103.
- Bandeira, S.O., 2002. Diversity and distribution of seagrasses around Inhaca Island, southern Mozambique. *S. Afr. J. Bot.* 68, 191–198. [https://doi.org/10.1016/S0254-6299\(15\)30419-1](https://doi.org/10.1016/S0254-6299(15)30419-1).
- Bandeira, S., Gullström, M., Balidy, H., Samussone, D., Cossa, D., 2014. Seagrass meadows in Maputo Bay. In: Bandeira, S., Paula, J. (Eds.), *The Maputo Bay Ecosystem*. WIOMSA, Zanzibar Town, Tanzania, pp. 147–169.
- Bandeira, S., Amone-Mabuto, M., Chitara-Nhandimo, S., Scarlet, M.P., Rafael, J., 2021. Impact of cyclones and floods on seagrass habitats. In: Nhamo, G., Chikodzi, D. (Eds.), *Cyclones in Southern Africa, 3. Implications for the Sustainable Development Goals Series*, pp. 279–288.
- Bakirman, T., Gumusay, M.U., 2020. Assessment of machine learning methods for seagrass classification in the Mediterranean. *Balt. J. Mod. Comput.* 8, 315–326. <https://doi.org/10.22364/bjmc.2020.8.2.07>.
- Benmokhtar, S., Robin, M., Maanan, M., Boutoumit, S., Badaoui, B., Bazairi, H., 2023. Monitoring the spatial and interannual dynamic of *Zostera noltei*. *Wetlands* 43, 16. <https://doi.org/10.1007/s13157-023-01690-7>.
- Calleja, F., Galván, C., Silió-Calzada, A., Juanes, J.A., Ondiviela, B., 2017. Long-Term analysis of *Zostera noltei*: A retrospective approach for understanding seagrasses' dynamics. *Mar. Environ. Res.* 130, 93–105. <https://doi.org/10.1016/j.marenvres.2017.07.017>.
- Chayhard, S., Buranapratheprath, A., 2018. Application of unmanned aerial vehicle to estimate seagrass biomass in Kung Kraben Bay, Chanthaburi province, Thailand. *Int. J. Agric. Technol.* 14, 1107–1114.
- Chen, J., Sasaki, J., Guo, Z., Endo, M., 2023. UAV-based seagrass wrack orthophotos classification for estimating blue carbon. *Est. Coast. Shelf Sci.* 293, 108476.
- Congalton, R.G., Green, K., 2019. *Assessing the Accuracy of Remotely Sensed Data: Principles and Practices*, 3rd ed. CRC Press, Boca Raton, FL, USA. <https://doi.org/10.1201/9780429052729>.
- D'Agata, C., 2016. Social and ecological factors influencing small-scale fisheries in the Bay of Bazaruto, Mozambique. MSc Thesis, Stockholm University, Sweden.
- de Boer, W.F., 2000. Biomass dynamics of seagrasses and the role of mangroves and seagrass vegetation as different nutrient sources for an intertidal ecosystem. *Aquat. Bot.* 66, 225–239. [https://doi.org/10.1016/S0304-3770\(99\)00072-8](https://doi.org/10.1016/S0304-3770(99)00072-8).
- Dronova, I., 2015. Object-based image analysis in wetland research: a review. *Remote Sens* 7, 6380–6413. <https://doi.org/10.3390/rs70506380>.
- Duarte, C.M., 1991. Allometric scaling of seagrass form and productivity. *Mar. Ecol. Prog. Ser.* 77, 289–300.
- Duffy, J.P., Pratt, L., Anderson, K., Land, P.E., Shutler, J.D., 2018. Spatial assessment of intertidal seagrass meadows using optical imaging systems and a lightweight drone. *Est. Coast. Shelf Sci.* 200, 169–180. <https://doi.org/10.1016/j.ecss.2017.11.001>.
- ESRI, 2020. ArcGIS Desktop: Release 10.8. Environmental Systems Research Institute: Redlands, CA, USA.
- Ferreira, M.A., Bandeira, S., 2014. Maputo Bay's coastal habitats. In: Bandeira, S., Paula, J. (Eds.), *The Maputo Bay Ecosystem*, vol. WIOMSA, Zanzibar Town, Tanzania, pp. 21–24.
- Ferreira, M.A., Andrade, F., Bandeira, S.O., Cardoso, P., Mendes, R.N., Paula, J., Mondlane, U.E., 2009. Analysis of cover change (1995 - 2005) of Tanzania/Mozambique trans-boundary mangroves using Landsat imagery. *Aquat. Conserv. Mar. Freshw.* 19, 38–45. <https://doi.org/10.1002/aqc.1042>.
- Ferreira, M.A., Andrade, F., Nogueira, M., Paula, R., 2012. Use of satellite remote sensing for coastal conservation in the Eastern African Coast: Advantages and shortcomings. *Eur. J. Remote Sens* 45. <https://doi.org/10.5721/EuJRS20124526>.
- Findlay, K.P., Cockcroft, V.G., Guissamulo, A.T., 2011. Dugong abundance and distribution in the Bazaruto Archipelago, Mozambique. *Afr. J. Mar. Sci.* 33, 441–452. <https://doi.org/10.2989/1814232X.2011.637347>.
- Gokulakrishnan, R., Ravikumar, S., 2016. Assessment of seagrass biomass and coastal land forms along Palk Strait. *Indian J. Geo-Mar. Sci.* 45, 1035–1041.
- Green, E.P., Short, F.T., 2003. *World Atlas of Seagrasses*. University of California Press, Berkeley, USA, p. 324.
- Guissamulo, A., Cockcroft, V.G., 2004. Ecology and population estimates of Indo-Pacific Humpback Dolphins (*Sousa chinensis*) in Maputo Bay, Mozambique. *Aquat. Mamm.* 30, 94–102. <https://doi.org/10.1578/am.30.1.2004.94>.
- Gullström, M., Dahl, M., Linden, O., Vorhies, F., Forsberg, S., Ismail, R.O., M., 2021. Coastal blue carbon stocks in Tanzania and Mozambique: support for climate adaptation and mitigation actions. *International Union for Conservation of Nature*. IUCN, p. 69.
- Hamad, I.Y., Staehr, P.A.U., Rasmussen, M.B., Sheikh, M., 2022. Drone-based characterization of seagrass habitats in the tropical waters of Zanzibar. *Remote Sens* 14, 680. <https://doi.org/10.3390/rs14030680>.
- Ivajnsić, D., Orlando-Bonaca, M., Doña, D., Grujić, V.J., Trkov, D., Mavrić, B., Lipej, L., 2022. Evaluating seagrass meadow dynamics by integrating field-based and remote sensing techniques. *Plants* 11, 1196. <https://doi.org/10.3390/plants11091196>.
- Kilminster, K., McMahon, K., Waycott, M., Kendrick, G.A., Scanes, P., McKenzie, L., O'Brien, K.R., Lyons, M., Ferguson, A., Maxwell, P., Glasby, T., Udy, J., 2015. Unravelling complexity in seagrass systems for management: Australia as a microcosm. *Sci. Total Environ.* 534, 97–109. <https://doi.org/10.3390/plants11091196>.
- Klemas, V., 2015. Coastal and environmental remote sensing from unmanned aerial vehicles: an overview. *J. Coast. Res.* 31, 1260–1267. <https://doi.org/10.2112/JCOASTRES-D-15-00005.1>.
- Knowles, A.K., Hillier, A., 2008. *Placing history: how maps, spatial data, and GIS are changing historical scholarship*. ESRI Press, p. 313.
- Koedwin, W., Intararuang, W., Ritchie, R.J., Huete, A., 2016. An integrated field and remote sensing method for mapping seagrass species, cover, and biomass in southern Thailand. *Remote Sens* 8, 292. <https://doi.org/10.3390/rs8040292>.
- Kuhwald, K., Schneider Von Deimling, J., Schubert, P., Oppelt, N., 2021. How can Sentinel-2 contribute to seagrass mapping in shallow, turbid Baltic Sea waters? *Remote Sens. Ecol. Conserv* 8, 328–346. <https://doi.org/10.1002/rse2.246>.
- Kutser, T., Hedley, J., Giardino, C., Roelfsema, C., Brando, V.E., 2020. Remote sensing of shallow waters — a 50 year retrospective and future directions. *Remote Sens. Environ.* 240, 111619. <https://doi.org/10.1016/j.rse.2019.111619>.

- Lechner, A.M., Fletcher, A., Johansen, K., Erskine, P., 2012. Characterising upland swamps using object-based classification methods and hyper-spatial resolution imagery derived from an unmanned aerial vehicle. *ISPRS Ann. Photogramm. Remote Sens. Spat. Inf. Sci.* 1–4, 101–106. <https://doi.org/10.5194/isprsannals-1-4-101-2012>.
- Li, Y., Bai, J., Chen, S., Chen, B., Zhang, L., 2023. Mapping seagrasses on the basis of Sentinel-2 images under tidal change. *Mar. Environ. Res.* 185, 105880. <https://doi.org/10.1016/j.marenvres.2023.105880>.
- Lønborg, C., Thomasberger, A., Stæhr, P.A.U., Stockmarr, A., Sengupta, S., Rasmussen, M.L., Nielsen, L.T., Hansen, L.B., Timmermann, K., 2021. Submerged aquatic vegetation: overview of monitoring techniques used for the identification and determination of spatial distribution in European coastal waters. *Integr. Environ. Assess. Manag.* 18, 892–908. <https://doi.org/10.1002/ieam.4552>.
- Lugendo, B., Wegoro, J., Shaghude, Y., Pamba, S., Makemie, M., Hollander, J., 2024. Seagrass mapping along the coast of Tanzania. *Ocean Coast. Manag.* 253, 107169. <https://doi.org/10.1016/j.ocecoaman.2024.107169>.
- Mahdavi, S., Salehi, B., Granger, J., Amani, M., Brisco, B., Huang, W., 2017. Remote sensing for wetland classification: a comprehensive review. *GISci. Remote Sens.* 55, 623–658. <https://doi.org/10.1080/15481603.2017.1419602>.
- Malerba, M.E., de Paula Costa, M.D., Friess, D.A., Schuster, L., Young, M.A., Lagomasino, D., Serrano, O., Hickey, S.M., York, P.H., Racheed, M., Lefcheck, J.S., Radford, B., Atwood, T.B., Lerodiaconou, D., Macreadie, P., 2023. Remote sensing for cost-effective blue carbon accounting. *Earth-Sci. Rev.* 238, 104337. <https://doi.org/10.1016/j.earscirev.2023.104337>.
- Mallombasi, A., Mashoreng, S., La Nafie, Y.A., 2020. The relationship between seagrass *Thalassia hemprichii* percentage cover and their biomass. *J. Ilmu Kelaut. SPERMONDE* 6, 7–10. <https://doi.org/10.20956/jiks.v6i1.9922>.
- Manfreda, S., McCabe, M.F., Miller, P.E., Lucas, R., Pajuelo, V.M., Mallinis, G., Ben Dor, E., Helman, D., Estes, L., Ciraolo, G., Müllerová, J., Tauro, F., De Lima, M.L., De Lima, J.L.M.P., Maltese, A., Frances, F., Caylor, K., Kohv, M., Perks, M., Ruiz-Pérez, G., Su, Z., Vico, G., Toth, B., 2018. Use of unmanned aerial systems for environmental monitoring. *Remote Sens.* 10, 641. <https://doi.org/10.3390/rs10040641>.
- Maxwell, A.E., Warner, T.A., Fang, F., 2018. Implementation of machine-learning classification in remote sensing: an applied review. *Int. J. Remote Sens.* 39, 2784–2817. <https://doi.org/10.1080/01431161.2018.1433343>.
- McKenzie, L.J., Finkbeiner, M.A., Kirkman, H., 2001. Methods for mapping seagrass distribution. In: Short, F.T., Coles, R.G. (Eds.), *Global Seagrass Research Methods*. Elsevier Science B.V., Amsterdam, pp. 101–121.
- Medina, J.A., Atehortúa, B.E.A., 2019. Comparison of maximum likelihood, support vector machines, and random forest techniques in satellite images classification. *Tecnura* 23, 59. <https://doi.org/10.14483/22487638.14826>.
- Nahirmick, N.K., Reshitnyk, L., Campbell, M., Hessler-Lewis, M., Costa, M., Yakimishyn, J., Lee, L., 2019. Mapping with confidence; delineating seagrass habitats using Unoccupied Aerial Systems (UAS). *Remote Sens. Ecol. Conserv.* 5, 121–135. <https://doi.org/10.1002/rse2.98>.
- Nordlund, L.M., Gullström, M., 2013. Biodiversity loss in seagrass meadows due to local invertebrate fisheries and harbour activities. *Est. Coast. Shelf Sci.* 135, 231–240. <https://doi.org/10.1016/j.ecss.2013.10.019>.
- Novak, A., Ostash, V., 2022. Digitizing historical maps and their presentation in online map collections. *e-Perimetro* 17, 33–44.
- Otuke, J.R., Blaschke, T., 2010. Land cover change assessment using decision trees, support vector machines and maximum likelihood classification algorithms. *Int. J. Appl. Earth Obs. Geoinf.* 12, S27–S31. <https://doi.org/10.1016/j.jag.2009.11.002>.
- Poursanidis, D., Traganos, D., Teixeira, L., Shapiro, A., Muaves, L., 2021. Cloud-native seascape mapping of Mozambique's Quirimbas National Park with Sentinel-2. *J. Remote Sens. Ecol. Conserv.* 7, 275–291. <https://doi.org/10.1002/rse2.187>.
- Price, D.M., Felgate, S.L., Huvenne, V.A.I., Strong, J., Carpenter, S., Barry, C., Lichtschlag, A., Sanders, R., Carrias, A., Young, A., Andrade, V., Cobb, E., Le Bas, T., Brittain, H., Evans, C., 2022. Quantifying the intra-habitat variation of seagrass beds with Unoccupied Aerial Vehicles (UAVs). *Remote Sens.* 14, 480. <https://doi.org/10.3390/rs14030480>.
- Pu, R., Bell, S., Meyer, C., Baggett, L., Zhao, Y., 2012. Mapping and assessing seagrass along the Western Coast of Florida using Landsat TM and EO-1 ALI/Hyperion Imagery. *Est. Coast. Shelf Sci.* 115, 234–245. <https://doi.org/10.1016/j.ecss.2012.09.006>.
- Purvaja, R., Robin, R., Ganguly, D., Hariharan, G., Singh, G., Raghuraman, R., Ramesh, R., 2018. Seagrass meadows as proxy for assessment of ecosystem health. *Ocean Coast. Manag.* 159, 34–45. <https://doi.org/10.1016/j.ocecoaman.2017.11.026>.
- Rao, R., Alcoverro, T., Kongari, P., Yoayela, S., Arthur, R., D'Souza, E., 2023. Tolerance to aerial exposure influences distributional patterns in multi-species intertidal seagrass meadows. *Mar. Environ. Res.* 191, 106146. <https://doi.org/10.1016/j.marenvres.2023.106146>.
- Roca, G., Alcoverro, T., Krause-Jensen, D., Balsby, T.J.S., van Katwijk, M.M., Marbà, N., Santos, R., Arthur, R., Mascaró, O., Fernández-Torquemada, Y., Pérez, M., Duarte, C. M., Romero, J., 2016. Response of seagrass indicators to shifts in environmental stressors: a global review and management synthesis. *Ecol. Indic.* 63, 310–323. <https://doi.org/10.1016/j.ecolind.2015.12.007>.
- Román, A., Tovar-Sánchez, A., Olivé, I., Navarro, G., 2021. Using a UAV-Mounted multispectral camera for the monitoring of marine macrophytes. *Front. Mar. Sci.* 8, 722698. <https://doi.org/10.3389/fmars.2021.722698>.
- Rommel, E., Giese, L., Fricke, K., Kathöfer, F., Heuner, M., Mölter, T., Deffert, P., Asgari, M., Nätke, P., Dzunic, F., 2022. Very high-resolution imagery and machine learning for detailed mapping of riparian vegetation and substrate types. *Remote Sens.* 14, 954. <https://doi.org/10.3390/rs14040954>.
- Short, F., Carruthers, T., Dennison, W., Waycott, M., 2007. Global seagrass distribution and diversity: a bioregional model. *J. Exp. Mar. Bio. Ecol.* 350, 3–20. <https://doi.org/10.1016/j.jembe.2007.06.012>.
- Singh, K.K., Frazier, A.E., 2018. A meta-analysis and review of unmanned aircraft system (UAS) imagery for terrestrial applications. *Int. J. Remote Sens.* 39, 5078–5098. <https://doi.org/10.1080/01431161.2017.142094>.
- Solana, G., Grifoll, M., Espino, M., 2020. Hydrographic variability and estuarine classification of Inhambane bay (Mozambique). *J. Coast. Res.* 95, 649–653. <https://doi.org/10.2112/SI95-126.1>.
- Traganos, D., Reinartz, P., 2018. Machine learning-based retrieval of benthic reflectance and *Posidonia oceanica* seagrass extent using a semi-analytical inversion of Sentinel-2 satellite data. *Int. J. Remote Sens.* 39, 9428–9452. <https://doi.org/10.1080/01431161.2018.1519289>.
- Traganos, D., Pertiwi, A.P., Lee, C.B., Blume, A., Poursanidis, D., Shapiro, A., 2022. Earth observation for ecosystem accounting: spatially explicit national seagrass extent and carbon stock in Kenya, Tanzania, Mozambique and Madagascar. *Remote Sens. Ecol. Conserv.* 6, 778–792.
- Uhrin, A.V., Townsend, P.A., 2016. Improved seagrass mapping using linear spectral unmixing of aerial photographs. *Est. Coast. Shelf Sci.* 171, 11–22. <https://doi.org/10.1016/j.ecss.2016.01.021>.
- Ventura, D., Grosso, L., Pensa, D., Casoli, E., Mancini, G., Valente, T., Scardi, M., Rakaj, A., 2023. Coastal benthic habitat mapping and monitoring by integrating aerial and water surface low-cost drones. *Front. Mar. Sci.* 9, 1096594. <https://doi.org/10.3389/fmars.2022.1096594>.
- Vieira, V.M.N.C.S., Lopes, I.E., Creed, J.C., 2018. The biomass-density relationship in seagrasses and its use as an ecological indicator. *BMC Ecol.* 18, 44. <https://doi.org/10.1186/s12898-018-0200-1>.
- Villoslada, M., Bergamo, T.F., Ward, R.D., Burnside, N.G., Joyce, C.B., Bunce, R.G.H., Sepp, K., 2020. Fine scale plant community assessment in coastal meadows using UAV based multispectral data. *Ecol. Indic.* 111, 105979. <https://doi.org/10.1016/j.ecolind.2019.105979>.
- Yang, B., Hawthorne, T.L., Aoki, L., Beatty, D.S., Copeland, T., Domke, L.K., Eckert, G.L., Gomes, C.P., Graham, O.J., Harvell, C.D., 2023. Low-altitude UAV imaging accurately quantifies eelgrass wasting disease from Alaska to California. *Geophys. Res. Lett.* 50. <https://doi.org/10.1029/2022GL101985>.